Research Square

Preprints are preliminary reports that have not undergone peer review.
They should not be considered conclusive, used to inform clinical practice,
or referenced by the media as validated information.

# Effects of Artisanal Monazite and Cassiterite Mining in the Amazon on Uranium and Thorium Concentrations

**Maria Kalyane Farias Silva**

kalyanefar@gmail.com

Universidade Federal Rural da Amazônia

**Edna Santos Souza**

Federal University of Southern and Southeastern Pará

**Research Article**

**Keywords:** Mining residues, radionuclides, contamination, ecological risk

**Posted Date:** November 11th, 2026

**DOI:** https://doi.org/10.21203/rs.3.rs-11225604/v1

**License:** This work is licensed under a Creative Commons Attribution 4.0 International License.
Read Full License

**Additional Declarations:** No competing interests reported.

# Abstract

Artisanal monazite and cassiterite mining can alter soil properties and promote the accumulation of naturally occurring radionuclides, such as uranium (U) and thorium (Th), in the generated mining residues. This study aimed to quantify U and Th concentrations and assess the potential for contamination and ecological risk in tailings and overburden from artisanal mining areas in the municipality of São Félix do Xingu, Pará, Brazil. Samples were collected from seven areas, including active mining sites, inactive areas, and natural forest soil as a reference. Chemical and particle-size properties, as well as U and Th concentrations, were determined. Contamination was assessed using the contamination factor (CF), enrichment factor (EF), geoaccumulation index (Igeo), and pollution load index (PLI), complemented by Spearman correlation analysis and principal component analysis. U and Th concentrations were higher in the mining materials than in the reference area, particularly in the tailings from the area inactive for 10 years, which showed the highest concentrations. The CF values indicated moderate contamination, whereas the EF indicated minimal enrichment. The Igeo classified the materials as unpolluted to slightly polluted, while the PLI indicated pollution in the mining areas. The results demonstrate the persistence of radionuclides in mining residues even after mining activities have ceased, reinforcing the need for environmental monitoring and remediation strategies.


# INTRODUCTION

Mining is an important source of resources that can promote a country's socioeconomic progress (Wu et al. 2021a). From this perspective, the Amazon holds the greatest mineral potential in Brazil and one of the most significant in the world, and the exploitation of the various mineral reserves in this region contributes to regional and national economic development (Caitano et al. 2021; Moia et al. 2024). However, this activity can also have significant negative impacts. The conversion of vegetation in the Amazon into agricultural, livestock, and artisanal mining areas is increasing, with 99% (3,279 ha) of the area deforested due to artisanal mining in 2024 located in the Amazon, particularly in the state of Pará (MapBiomas 2025). Furthermore, artisanal mining methods have low mineral extraction efficiency and generate large amounts of tailings, as more than 10 billion tons of tailings are produced worldwide each year (Zhao et al. 2023).

Mineral production is responsible for a range of environmental impacts, mainly associated with soil and water contamination by heavy metals and other toxic elements, such as the naturally occurring radionuclides uranium (U) and thorium (Th) (Vengosh et al. 2022; Zhao et al. 2023). These effects are related to the role of water and sediments as the main pathways for pollutant storage, through which contaminants can accumulate over time and be released into the environment when environmental conditions change. Consequently, these contaminants can affect human health and pose ecological risks through the food chain, particularly through the consumption of contaminated water and food (Pedrozo-Acuña et al. 2025).

Monazite and cassiterite are highly important mineral resources associated with different elements of economic interest (Li et al. 2023; Zhao et al. 2025). Monazite, with the formula (Ce,La,Y,Th)$PO_4$, is a rare earth element (REE)-rich phosphate of great relevance to high-value technological and industrial sectors, and it also contains uranium oxide ($U_3O_8$) and thorium oxide ($ThO_2$) in its composition (Kotb et al. 2023; Zhao et al. 2025). This mineral has a stable phosphate mineral structure, high phosphorus content, high radioactivity, and complex impurities, which make its decomposition a technological challenge because it requires specific processes for the extraction of REEs of economic interest. In addition, mineral processing generates radioactive waste that is harmful to the environment (Whang et al. 2026). Cassiterite ($SnO_2$) is the main tin-bearing mineral and has widespread industrial and technological applications (Li et al. 2023). A measurable U content is also present in its composition (Du et al. 2022). Furthermore, due to its high mechanical and chemical resistance, as well as its stability under weathering, cassiterite is an important indicator mineral for the characterization of the parent rock (Nwamba et al. 2023).

Uranium and thorium are referred to as naturally occurring radionuclides or radioelements, which belong to the actinide series in the periodic table and are among the contaminants that may be present in mineral tailings. These radioelements are the only members of this group that occur naturally, with concentrations in the Earth's crust ranging from 2 to 3 ppm for uranium and from 8 to 12 ppm for thorium (Melquiades et al. 2024). The release of these elements into the environment results from mineral processing activities, as well as from the manufacture and excessive use of phosphate fertilizers (Braz et al. 2021).

Thorium has a wide range of applications, particularly in enhancing the resistance of certain materials, as a coating for electronic devices, in lighting, in high-quality camera lenses, and in nuclear technology (Kaynar et al. 2021). Uranium, in turn, is considered a valuable commodity and serves as a raw material for the production of fuel for nuclear power plants used for baseload electricity generation (Joel and Shop 2026).

U and Th concentrations in soil vary according to geological formation, physical characteristics, topographic differences, geomorphology, and weather conditions in the region (Martín et al. 2025). At low natural levels, naturally occurring radioactive materials do not pose risks; however, increased anthropogenic activities, such as deep soil excavation caused by mining, can increase their concentrations in the environment (Ankapong et al. 2024). The accumulation of mining waste in open areas increases the risk of pollution by these elements because they can be easily dispersed through leaching, weathering, or leakage, causing contamination of water bodies and soil (Wu et al. 2021b).

The region that includes the municipality of São Félix do Xingu, Pará, in the Brazilian Amazon, has extensive areas of artisanal monazite and cassiterite mining, where large amounts of tailings are produced that may cause ecological and health damage. Therefore, this study aimed to quantify U and Th levels and estimate the ecological risk of tailings and overburden from artisanal monazite and

cassiterite mining areas, as well as to analyze the relationships between radioelement concentrations and soil attributes.

## MATERIALS AND METHODS

# Study Area

The study area is located in the municipality of São Félix do Xingu (06°37'48" S and 51°57'36" W), in the southeastern region of the state of Pará, within the Brazilian Amazon. The region has a predominantly humid tropical climate, classified as Am according to the Köppen classification, with an average annual temperature of 26°C (Alvares et al. 2013). Total annual precipitation is 1,734 mm, with the highest rainfall intensity occurring from November to April.

The municipality is located in the south-central portion of the Amazonian Craton, characterized by extensive deposits of volcanic and volcaniclastic origin associated with subvolcanic bodies and Paleoproterozoic plutonic intrusions. The rocks have well-preserved textures and structures (Cruz et al. 2014). São Félix do Xingu is drained mainly by the Xingu River and other rivers, such as the Fresco River (Claudino et al. 2020). The forest formation is classified as ombrophilous forest, occurring in open and dense forms (Fapespa 2023).

## Sampling

Samples were collected using a stainless-steel Dutch auger. To avoid contamination, samples were collected at a depth of 0–0.2 m. Five individual samples were collected to form one composite sample (approximately 2.5 kg). The material was then passed through a 2-mm-mesh sieve, air-dried, and stored in polyethylene bags until analysis.

Samples were obtained from seven areas identified as follows: AO1 = overburden from active mines (10 samples); AT1 = tailings from active mines (8 samples); AO2 = overburden from mines deactivated for one year (4 samples); AT2 = tailings from mines deactivated for one year (3 samples); AO3 = overburden from mines deactivated for ten years (4 samples); AT3 = tailings from mines deactivated for ten years (3 samples); and FN = natural forest soil (3 samples), considered the reference (Fig. 1).

## Sample Properties

The chemical and particle-size properties of the soil and mining residues were determined according to the methodology described by Teixeira et al. (2017). Soil pH was determined in water using a potentiometer (Thermo Scientific) at a soil-to-water ratio of 1:2.5. Available phosphorus (P) and potassium ($K^+$) were extracted with Mehlich-1 solution, and their concentrations were determined by colorimetry and flame photometry, respectively. Exchangeable calcium ($Ca^{2+}$) and magnesium ($Mg^{2+}$) were extracted with 1 M KCl solution, and their concentrations were determined by atomic absorption

spectrophotometry. Cation exchange capacity (CEC) was calculated from the sum of the exchangeable concentrations of $Ca^{2+}$, $Mg^{2+}$, $K^{+}$, and $Al^{3+}$. Organic carbon (OC) content was determined by wet combustion with potassium dichromate, and the values obtained were multiplied by 1.72 to determine organic matter (OM) content. Soil texture was characterized using the pipette method (Gee and Bauder 1986).

The concentrations of U and Th were extracted in triplicate using the alkaline fusion method according to Pereira et al. (2023), and their concentrations were determined by inductively coupled plasma mass spectrometry (ICP-MS, PerkinElmer), as were the Fe concentrations used to calculate the pollution indices. Blank samples and certified reference material (GRE-3®) were included for analytical quality control.

## Contamination and Risk Assessment

The geoaccumulation index (Igeo), contamination factor (CF), enrichment factor (EF), and pollution load index (PLI) were used to determine the contamination levels of naturally occurring radionuclide elements, while the potential ecological risk factor (PERF) and potential ecological risk index (PERI) were used to assess ecological risk (Khan et al. 2020; Pereira et al. 2023; Musiige et al. 2024). Details of the indices are presented below.

Contamination Factor (CF)

This index represents contamination resulting from the addition of elements due to human activities and was calculated according to Eq. (1):

$$CF = \frac{C_E}{B_E}$$

1

Where CE is the mean concentration of the element in the mining area, and BE is the concentration of the same element in the reference area. The results were interpreted according to Hakanson (1980), where CF < 1 represents low contamination; CF between 1 and 3 represents moderate contamination; CF between 3 and 6 represents considerable contamination; and CF > 6 represents high contamination.

Enrichment Factor

The EF is used to calculate the degree of enrichment of the studied radioelements in the area and, thus, allows the assessment of contamination in an anthropogenically impacted area relative to a reference area, considering a reference element. Al, Ca, Fe, Mn, Ti, and V are commonly used as reference elements (Braz et al. 2021). Iron was used as the conservative element in this study. This index was calculated using the following Eq. (2):

$$EF = \left(\frac{C_n}{C_r}\right) / \left(\frac{B_n}{B_r}\right)$$

2

Where Cn is the concentration of U or Th in the impacted area, Cr is the Fe concentration in the same area, Bn is the concentration of U or Th in the reference area, and Br is the Fe concentration in the same area. The EF values were interpreted as follows: EF < 2 indicates minimal enrichment; EF between 2 and 5 represents moderate enrichment; EF between 5 and 20 indicates significant enrichment; EF between 20 and 40 indicates very high enrichment; and EF > 40 indicates extremely high enrichment (Sutherland 2000).

Geoaccumulation Index (Igeo)

The Igeo is used to assess the current degree of element pollution relative to the natural environment. The geoaccumulation index (Igeo) was calculated based on Eq. (3), as proposed by Müller et al. (1979).

$$Igeo = Log_2\left(\frac{C_n}{1{,}5B_n}\right)$$

3

Where Cn represents the concentration of U or Th in this study, Bn is the concentration of the same elements in the reference area, and 1.5 is a constant used to account for the effects of lithogenic variations in the data. The Igeo was interpreted as follows: Igeo ≤ 0 indicates unpolluted soil; Igeo between 0 and 1 indicates slightly polluted soil; Igeo between 1 and 2 indicates moderately polluted soil; Igeo between 2 and 3 indicates moderately to strongly polluted soil; Igeo between 3 and 4 indicates strongly polluted soil; Igeo between 4 and 5 indicates strongly to extremely polluted soil; and Igeo > 5 indicates extremely polluted soil (Nkinahamira et al. 2019).

Pollution Load Index (PLI)

The PLI is commonly used to estimate the cumulative contamination by potentially toxic elements in soils. It is calculated from the contamination factors obtained using Eq. (4).

$$PLI = (CF_1 X CF_2 X \dots CF_n)^{\frac{1}{n}}$$

4

Where CF represents the contamination factor and n corresponds to the number of elements analyzed. The pollution index (PLI) values were classified according to Tomlinson et al. (1980) as follows: PLI ranging from 0 to 1 indicates no pollution, whereas PLI > 1 indicates polluted material.

# Statistical Analyses

The data were subjected to descriptive statistics, and data normality was assessed using the Shapiro–Wilk test ($p < 0.05$). The data did not follow a normal distribution; therefore, Spearman correlation analysis was performed for nonparametric data, along with principal component analysis (PCA) to explore the relationships between U and Th concentrations and soil and mining residue properties. All analyses were performed using R software version 4.3.3 (R Core Team 2023).

## RESULTS

# Soil Physicochemical Characterization

The particle size analysis showed a predominance of the sand fraction in most areas. Clay content ranged from approximately 18.6% to 41.2%. Mining residues from active artisanal mining areas had lower clay contents than those from the other areas and the reference site. In particular, tailings from the active mining area had the lowest clay content and the highest sand proportion (Table 1). Soil particle size directly influences the retention or release of metals in mining residues. Thus, coarser particles promote acid production and cause the release of metals into the environment. In contrast, finer particles, due to their greater specific surface area, favor water retention, binding to organic matter, and soil aggregate formation. Therefore, residues with higher clay content are more amenable to rehabilitation (Li et al. 2022; Li et al. 2024). Consequently, the particle size heterogeneity of these materials is relevant to the environmental assessment of ASGM areas, given that particle size directly influences the retention, mobility, and availability of potentially toxic elements (PTEs) in soil.

The pH ranged from 4.6 to 4.9, indicating acidic conditions, even in the reference area (Table 1). Acidity in mining residues may be associated with the oxidation of sulfide minerals exposed during mining activities. Minerals such as pyrite ($FeS_2$), when exposed to oxygen and water, undergo oxidation reactions that generate sulfuric acid and $H^+$, resulting in a decrease in pH (Mogashane et al. 2025; Otunola and Mhangara 2024). These acidic conditions can persist for long periods, even after mining activities cease, due to the persistence of these reactions and continued material exposure. This was also observed in the present study, in which inactive mining areas still exhibited low pH values (Keller et al. 2025). These conditions significantly affect the solubility, availability, and migration of these elements in soil, making them available for plant uptake and promoting contamination of other areas and water bodies (Xu et al. 2023).

The acidity of natural soils is consistent with that reported for tropical soils, which are naturally acidic due to parent materials with low base cation contents and intense leaching of these elements under the region's high rainfall conditions (Agegnehu et al. 2021; Mahecha-Pulido et al. 2025). Furthermore, these reactions may be intensified by water percolation, which increases base removal and accelerates weathering processes, while also contributing to the persistence of the natural acidity of Amazonian soils (Xu et al. 2023). In the Brazilian Amazon, particularly in the state of Pará, forest soils with pH values below 5 have been reported, consistent with the pedogenetic characteristics of Amazonian soils developed from highly weathered parent materials (Gonçalves et al. 2022; Lima et al. 2022).

Soil pH directly influences the mobility and availability of U in soil, as its mobility and availability for plant uptake increase under acidic conditions, unlike Th, which has limited mobility due to its strong sorption to soil particles (Cui et al. 2022; Patel et al. 2023). The relationship between pH and U mobility in soil is associated with the high $H^+$ concentration in the soil solution under acidic conditions. Thus, $H^+$ ions occupy active sites on colloid surfaces, reducing adsorption, which increases U mobility and may facilitate its loss through leaching (Wang et al. 2024).

P content in the study areas ranged from 0.73 to 1.94 in tailings and overburden, whereas the value in the reference area was almost twice as high. These results may be related to greater organic matter accumulation in FN, since its presence in soil can increase P availability by promoting mineralization and reducing the adsorption of anions, such as phosphate, due to its predominantly negative charges (Monicelli et al. 2021; Jindo et al. 2023). This interpretation is supported by the higher OC contents in FN compared with the artisanal mining areas, with values approximately three to 16 times higher. Land-use changes frequently result in OC losses (Beillouin et al. 2023).

CEC values were also higher in the reference area. The low CEC in mining residues indicates their lower capacity to retain exchangeable cations, which is also related to reduced organic matter inputs associated with the lack of vegetation cover in mined areas. This is because increased OC is directly associated with higher CEC, as the functional groups of organic matter carry negative charges capable of adsorbing and exchanging cations. Thus, carbon inputs into the soil are reduced, and the lower OC values found in mining residues support this interpretation (Bi et al. 2023; Alarcón-Aguirre et al. 2023). High rainfall and temperatures in the Amazon region, together with washing during mineral processing, favor base cation losses and low CEC. Furthermore, these conditions promote environmental contamination, since organic matter is a major contributor to CEC, and its low levels increase the risk of PTE leaching due to the reduced cation retention capacity (Raso et al. 2022; Nahum et al. 2024).

Table 1
Chemical properties and particle size distribution of soils and mining residues in the study areas.

| pH | AO1 | AT1 | AO2 | AT2 | AO3 | AT3 | FN |
|---|---|---|---|---|---|---|---|
| | **4,55 ± 0,12** | **4,50 ± 0,25** | **4,54 ± 0,16** | **4,67 ± 0,09** | **4,68 ± 0,25** | **4,86 ± 0,02** | **4,78 ± 0,11** |
| P | 1,37 ± 0,94 | 1,55 ± 0,87 | 1,51 ± 0,53 | 1,94 ± 0,75 | 1,23 ± 0,63 | 0,73 ± 0,28 | 3,30 ± 0,14 |
| SB | 0,54 ± 0,14 | 0,50 ± 0,32 | 0,69 ± 0,03 | 0,50 ± 0,11 | 0,49 ± 0,37 | 0,39 ± 0,17 | 1,36 ± 0,03 |
| CEC | 1,53 ± 0,72 | 0,98 ± 0,54 | 1,11 ± 0,56 | 1,01 ± 0,39 | 1,34 ± 0,78 | 0,78 ± 0,44 | 2,34 ± 0,05 |
| OC | 11,10 ± 9,33 | 7,47 ± 12,7 | 5,37 ± 7,16 | 23,70 ± 2,18 | 22,20 ± 12,30 | 9,42 ± 3,18 | 87,40 ± 65,60 |
| Clay (mg) | 209 ± 176 | 186 ± 198 | 235 ± 136 | 412 ± 221 | 314 ± 231 | 212 ± 32,60 | 305 ± 8,49 |
| Sand (mg) | 687 ± 223 | 742 ± 261 | 597 ± 326 | 475 ± 272 | 407 ± 44,80 | 681 ± 48,70 | 370 ± 3,54 |
| Silt (mg) | 79,30 ± 102 | 50,60 ± 64,30 | 82,90 ± 192 | 115 ± 57,50 | 134 ± 275 | 101 ± 46,40 | 320 ± 4,95 |

OM Organic matter, CEC Cation exchange capacity

# Radioelement Concentrations

U and Th concentrations in the artisanal mining areas were higher than those in the reference area, with Th concentrations approximately four times higher. The higher Th concentrations are associated with its greater abundance in monazite, one of the minerals widely exploited in artisanal mining activities in the study areas, and also reflect its higher natural abundance in the Earth's crust compared with U (Kotb et al. 2023; Melquiades et al. 2024). Additionally, it is worth noting that in the surface soil horizons, which are characterized by oxidizing conditions, uranium tends to occur in soluble forms, favoring its leaching and consequent environmental contamination. Its distribution is associated with soil fractions influenced by pH, redox conditions, and the presence of organic compounds, whereas Th was found to be irreversibly retained by soil particles (Xie et al. 2024; Porto et al. 2026). The concentrations of these elements were similar among the artisanal mining areas, with the highest concentrations of both elements observed in AT3, while the lowest concentrations were found in FN. Therefore, the concentrations of radioelements in this study may be considered to be controlled by the pollution source, with higher concentrations occurring closer to the source. The elevated concentrations identified in the tailings and overburden reinforce their anthropogenic origin associated with mining waste deposition, whereas the reference area represents natural background levels (Table 2).

Table 2
Uranium and thorium concentrations in the study areas.

| | AO1 | AT1 | AO2 | AT2 | AO3 | AT3 | FN |
|---|---|---|---|---|---|---|---|
| **mg.kg$^{-1}$** | | | | | | | |
| U | 4,32 ± 3,53 | 6,36 ± 19,10 | 6,37 ± 11,60 | 4,21 ± 31,10 | 3,48 ± 4,22 | 6,63 ± 2,96 | 2,92 ± 0,813 |
| Th | 20,20 ± 16,10 | 22,00 ± 157,00 | 25,90 ± 162,00 | 19,80 ± 236,00 | 20,90 ± 22,50 | 36,90 ± 15,30 | 12,80 ± 4,03 |

# Relationships Between Variables

Significant Spearman correlation coefficients were observed between the elements and soil and mining residue attributes. Strong and significant negative correlations were observed between sand and clay, as expected from the inverse relationship between these soil fractions. The same pattern was observed between sand and OC, which, in turn, showed a positive correlation with the clay and silt fractions. This behavior can be explained by the lower capacity of soils and mining residues dominated by the sand fraction to retain organic matter, facilitating its rapid decomposition and mineralization, whereas clay particles form stable aggregates with organic matter, protecting it from decomposition (Bi et al. 2023). Regarding chemical attributes, CEC showed significant positive correlations with potential acidity and the sum of bases, as expected, since it has exchange sites capable of retaining both the cationic nutrients represented by the sum of bases and acidic cations. For the radionuclides U and Th, a strong positive correlation was observed between them; in contrast, both showed significant negative correlations with the sum of bases (Fig. 2). The strong positive correlation between the radioelements indicates a common mineralogical origin, since monazite is one of the minerals exploited by artisanal mining in the study areas, and both radionuclides are associated with resistant minerals such as monazite (Kotb et al. 2023). Since the sum of bases is an indicator of soil fertility, its inverse relationship with the radioactive elements, represented by the negative correlation, is related to the fact that soils with higher U and Th concentrations are less fertile, as previously evidenced by the lower CEC, sum of bases, and OC observed in the mining residues. These residues possibly contain higher amounts of Fe and Al oxides, whose adsorption sites have a lower capacity to retain basic cations than organic matter, which is nearly absent in these areas (Strawn 2021).

Principal component analysis (PCA) was used to assess the relationship between the radioelements and the chemical properties of soils and mining residues in the study areas. The results showed that PCA explained 50.2% of the total data variability, with 29.5% explained by principal component one and 20.7% by principal component two. A strong relationship was observed between U and Th, due to the similar origin of these elements, with a greater association of these elements with sand content and potential acidity compared with the other soil attributes (Fig. 2). This closer relationship with the sand fraction may be related to the enrichment of the sandy fraction in heavy minerals containing U and Th, such as monazite itself, which has a high density and is generally associated with deposits of heavy mineral-rich

sands and extracted as a byproduct of this type of mining (Veerasamy et al. 2021; Dostal 2025). Furthermore, the relationship of these elements with potential acidity may be explained by the influence of soil acidity on their geochemical behavior, particularly U, whose mobility and availability may be altered under more acidic conditions (Patel et al. 2023).

a) b)

# Pollution Assessment Indices

The intensity of contamination was assessed using the CF, EF, Igeo, and PLI indices, presented in Table 3. The CF indicated moderate contamination by U and Th in all areas (Fig. 3), indicating the presence of these elements at levels that may already affect environmental quality, considering that this radiological risk, when combined with the low pH, low sum of bases, and limited organic matter conditions observed in the mining residues, increases their bioavailability (Bessa et al. 2024). The reference area showed lower values than the other areas; however, it was still classified as moderately contaminated. This may be related to the proximity of these areas to artisanal mining sites and sediment transport, considering the high rainfall in the Amazon region and the lack of vegetation cover in artisanal mining areas. In addition, this indicates that the local geology may be rich in U- and Th-bearing minerals, contributing to the levels observed in FN (Popoola et al. 2025). Higher CF values were found in the tailings from the mining area that had been inactive for 10 years. Some studies have shown that mining tailings commonly exhibit high CF values even after long periods of inactivity (Wang et al. 2021). Considering the PLI values, which ranged from 1.39 to 2.62 in the artisanal mining areas, the occurrence of pollution in these areas is further supported, whereas the reference area showed no pollution.

For the EF, the U and Th values indicated minimal enrichment, suggesting that their concentrations were similar to those in the reference area and that the predominant origin of these radioelements tends to be geogenic, that is, associated with natural processes such as mineral weathering, parent rock composition, and natural sediment transport (Patel et al. 2023; Martín et al. 2025). Furthermore, the high acidity and predominance of a sandy texture may have favored the solubilization, mobility, and leaching of these radioelements (Braz 2021).

The Igeo values showed variation in the degree of pollution, ranging from unpolluted to slightly polluted. For U, the overburden from active artisanal mining areas (AO1) and areas inactive for 10 years (AO3), the tailings from the mining area inactive for 1 year (AT2), and the soil from the reference area (FN) showed no pollution, whereas the other areas were classified as slightly polluted. In contrast, for Th, all artisanal mining areas were classified as slightly polluted by this element, whereas the reference area showed no soil pollution. This variation in U pollution among the areas may be related to evidence that this element is more sensitive to redox conditions. Under reducing conditions, U(IV), which is poorly soluble and readily precipitates, is formed, whereas under oxidizing conditions, U(VI), which is soluble, is formed; thus, greater heterogeneity in its distribution may occur (Mitra et al. 2025). The slight Th pollution in the mining residues is associated with its lower mobility, as it remains associated with minerals due to its

high positive charge ($Th^{4+}$) and the chemical stability of its host minerals. Therefore, Th tends to accumulate more in mining residues, resulting in higher Igeo values compared with U (Martín et al. 2025).

Table 3
Contamination factor (CF), enrichment factor (EF), geoaccumulation index (Igeo), and pollution load index (PLI) for U and Th.

| | U | | | Th | | | PLI |
|---|---|---|---|---|---|---|---|
| | CF | EF | IGEO | CF | EF | IGEO | |
| AO1 | 1,48 ± 1,21 | 1,51 ± 0,96 | -0,02 ± 0,77 | 1,57 ± 1,25 | 1,63 ± 1,07 | 0,06 ± 0,92 | 1,51 ± 1,20 |
| AT1 | 2,18 ± 6,57 | 0,66 ± 1,40 | 0,54 ± 1,42 | 1,71 ± 12,20 | 0,56 ± 2,13 | 0,19 ± 1,67 | 1,93 ± 8,98 |
| AO2 | 2,19 ± 3,98 | 1,51 ± 0,47 | 0,54 ± 1,42 | 2,02 ± 12,60 | 1,39 ± 1,94 | 0,43 ± 2,29 | 2,10 ± 7,24 |
| AT2 | 1,44 ± 10,7 | 1,37 ± 1,48 | -0,06 ± 2,26 | 1,54 ± 18,30 | 1,47 ± 2,95 | 0,04 ± 2,66 | 1,49 ± 14,00 |
| AO3 | 1,19 ± 1,45 | 0,78 ± 1,23 | -0,33 ± 1,10 | 1,63 ± 1,75 | 0,76 ± 1,47 | 0,12 ± 1,21 | 1,39 ± 1,59 |
| AT3 | 2,27 ± 1,02 | 0,30 ± 0,88 | 0,60 ± 0,84 | 2,87 ± 1,19 | 0,39 ± 0,83 | 0,94 ± 0,99 | 2,62 ± 1,07 |
| FN | 1,00 ± 0,28 | 1,01 ± 0,32 | -0,61 ± 0,41 | 1,00 ± 0,314 | 1,01 ± 0,35 | -0,62 ± 0,46 | 1,00 ± 0,30 |

*AO1: Active overburden; AT1: Active tailings; AO2: Inactive for 5 years overburden; AT2: Inactive for 5 years tailings; AO3: Long-term inactive overburden; AT3: Long-term inactive tailings; FN: Reference área.

*CF: Contamination factor; EF: Enrichment factor; Igeo: Geoaccumulation index; PLI: Pollution load index.

# Conclusion

This study examined U and Th pollution levels in artisanal monazite and cassiterite mining areas and the role of soil properties in this context. The data showed that artisanal mining activities directly influence the distribution of the radionuclides uranium and thorium in the environment. Tailings from the mining site with the longest period of inactivity showed the highest radionuclide concentrations and contamination levels, demonstrating that contamination may persist even after long periods of inactivity, although at minimal levels. The results of this study demonstrate that, despite the low anthropogenic contamination, artisanal mining increases environmental risks, highlighting the need for remediation measures to mitigate impacts in the medium and long term and prevent environmental risks, considering that mining residues and their weathering may contaminate water, soil, and groundwater with radioactive elements. The findings also reinforce the need to expand research by determining the fractions with

which U and Th are associated, in addition to conducting mineralogical analyses to better explain the retention of these elements. Furthermore, phytoremediation measures and soil amendments should be explored.

## Declarations

# Compliance with Ethical Standards

**Conflict of Interest**: The authors declare that they have no conflicts of interest.

# Author Contribution

MKFS: Data analysis and interpretation; manuscript writing;ESS: critical review of the manuscript; manuscript writing

# Data Availability

The authors declare that the data supporting the conclusions of this study are available in the article. If raw data files in another format are required, they can be obtained upon reasonable request from the corresponding author.

## References


1. Agegnehu G, Amede T, Erkossa T, Yirga C, Henry C, Tyler R, Sileshi GW (2021) Extent and management of acid soils for sustainable crop production system in the tropical agroecosystems: a review. Acta Agriculturae Scandinavica, Section B-Soil & Plant Science, 71(9): 852–869. https://doi.org/10.1080/09064710.2021.1954239
2. Alarcón-Aguirre G, Quispe ES, Zavaleta TV, Tejada LVP, Enciso DR, Achata LR, Garate-Quispe J (2023) Vegetation dynamics in lands degraded by gold mining in the southeastern Peruvian Amazon. Trees, Forests and People, Trees, Forests and People, 11: 100369. https://doi.org/10.1016/j.tfp.2023.100369.
3. Ankapong E, Gyamfi O, Agyei V, Dodd M, Akoto O, Darko G (2024) Soil-to-plant transfer factors of uranium and thorium in mining and non-mining districts of Ghana. Journal of Environmental Radioactivity, 280: 107566. https://doi.org/10.1016/j.jenvrad.2024.107566
4. Beillouin D, Corbeels M, Demenois J, Berre D, Boyer A, Fallot A, Feder F, Cardinael R (2023) A global meta-analysis of soil organic carbon in the Anthropocene. Nature Communications, 14(1): 3700. https://doi.org/10.1038/s41467-023-39338-z

5. Bessa AZE, Koutchouo MG, Doumo EPE, Manishimwe NK, Tanantsap RJN, Djoban JGT, Gouott BSB, Armstrong-Altrin JS (2024) Assessment of heavy metals and radionuclides (U and Th) contamination, and source identification of the Lékié Watershed sediments, Cameroon. Geosystems and Geoenvironment, 3(1): 100249. https://doi.org/10.1016/j.geogeo.2023.100249
6. Bi X, Chu H, Fu M, Xu D, Zhao W, Zhong Y, Zhang YN (2023). Distribution characteristics of organic carbon (nitrogen) content, cation exchange capacity, and specific surface area in different soil particle sizes. Scientific Reports, 13(1): 12242. https://doi.org/10.1038/s41598-023-38646-0
7. Braz AMS, Costa ML, Ramos SJ, Dall'Agnol R, Fernandes AR (2021) Long term application of fertilizers in Eastern Amazon and effect on uranium and thorium levels in soils. Minerals, 11(9): 994. https://doi.org/10.3390/min11090994
8. Caitano TBS, Ribeiro MM, Morales GP, Pontes AN (2021) Um panorama das receitas de direitos de mineração na Amazônia brasileira e reflexões sobre indicadores socioeconômicos. Revista Brasileira de Gestão e Desenvolvimento Regional, 17(1): 216–226. https://doi.org/10.54399/rbgdr.v17i1.6168
9. Claudino LSD, Ferreira LA, Poccard-Chapuis RJM (2020) Evolução dos sistemas agrários na microrregião de São Félix do Xingu (Amazônia brasileira): História e questões para pensar o desenvolvimento territorial. Revista DELOS, 13(36).
10. Cruz RS, Fernandes CMD, Juliani C, Lagler B, Misas CME, Nascimento TS, Jesus AJC (2014) Química mineral do vulcano-plutonismo paleoproterozoico da região de São Félix do Xingu (PA), Cráton Amazônico. Geologia USP. Série Científica, 14(1): 97–116. https://doi.org/10.5327/Z1519-874X201400010007
11. Cui Q, Zhang Z, Beiyuan J, Cui Y, Chen L, Chen H, Fang L (2022) A critical review of uranium in the soil-plant system: Distribution, bioavailability, toxicity, and bioremediation strategies. Critical Reviews in Environmental Science and Technology, 53(3): 340–365. https://doi.org/10.1080/10643389.2022.2054246
12. Dostal J (2025) Deposits of rare earth elements in Canada. FACETS, 10: 1–18. https://doi.org/10.1139/facets-2025-0148.
13. Du Y, Lu Y, Zhang Z, Fu J (2022) Indosinian magmatism and mineralization in the Banjiaoyuan tin deposit, middle Nanling Range, South China: Constraints from zircon and cassiterite U-Pb ages, geochemistry and Sr-Nd-Hf isotopic compositions. Ore Geology Reviews, 151: 105190. https://doi.org/10.1016/j.oregeorev.2022.105190
14. Fundação Amazônia de Amparo a Estudos e Pesquisas (FAPESPA). São Félix do Xingu: diagnóstico municipal. Belém: FAPESPA, ano. https://www.fapespa.pa.gov.br/wp-content/uploads/2025/02/Sao-Felix-do-Xingu.pdf. Acessado em 28 de janeiro de 2026.
15. Gonçalves DAM, Pereira WVS, Johannesson KH, Pérez DV, Guilherme LRG, Fernandes AR (2022) Geochemical background for potentially toxic elements in forested soils of the state of Pará, Brazilian Amazon. Minerals, 12(6): 674. https://doi.org/10.3390/min12060674.

16. Gee GW, Bauder JW (1986) Particle-size analysis. In: Klute A (ed) Methods of soil analysis. Part 1: Physical and mineralogical methods. 2nd ed. Madison: American Society of Agronomy; Soil Science Society of America, pp. 383–411.
17. Hakanson L (1980) An ecological risk index for aquatic pollution control: a sedimentological approach. Water Research, 14(8): 975–1001. https://doi.org/10.1016/0043-1354(80)90143-8.
18. Jindo K, Audette Y, Olivares FL, Canellas LP, Smith DS, Voroney RP (2023) Biotic and abiotic effects of soil organic matter on the phytoavailable phosphorus in soils: a review. Chemical and Biological Technologies in Agriculture, 10(1): 29. https://doi.org/10.1186/s40538-023-00401-y.
19. Shouop CJG (2026) Uranium at the nexus of energy security and sustainable development in a renuclearised world: demand trajectories and technological pathways. BMC Environmental Science, 3: 3. https://doi.org/10.1186/s44329-025-00045-3
20. Kaynar UH, Çam Kaynar S, Ekdal Karali E, Ayvacıklı M, Can N (2021) Adsorption of thorium (IV) ions by metal ion doped ZnO nanomaterial prepared with combustion synthesis: Empirical modelling and process optimization by response surface methodology (RSM). Applied Radiation and Isotopes, 178: 109955. https://doi.org/10.1016/j.apradiso.2021.109955.
21. Keller FS, Boff C, Silva D, Grigorieff A, Weber CC, Weiler J, Schneider IAH (2025) Attenuation of acid mine drainage in a coal waste deposit in Southern Brazil and the prospect of transitioning from active to passive treatment. Minerals, 15(10): 1068. https://doi.org/10.3390/min15101068
22. Khan R, Islam MS, Tareq ARM, Naher K, Islam ARMT, Habib MA, Siddique MAB, Islam MA, Das S, Rashid MB, Ullah AKMA, Miah MMH, Masrura SU, Bodrud-Doza M, Sarker MR, Badruzzaman ABM (2020) Distribution, sources and ecological risk of trace elements and polycyclic aromatic hydrocarbons in sediments from a polluted urban river in central Bangladesh. Environmental Nanotechnology, Monitoring & Management, 14: 100318. https://doi.org/10.1016/j.enmm.2020.100318
23. Kotb NA, Abd El Ghany MS, El-Sayed AA (2023) Radiological assessment of different monazite grades after mechanical separation from black sand. Scientific Reports, 13(1): 15389. https://doi.org/10.1038/s41598-023-42287-8.
24. Lemos RC de, Santos RD dos (1996) Manual de descrição e coleta de solo no campo. 3. ed. Campinas: Sociedade Brasileira de Ciência do Solo; Rio de Janeiro: EMBRAPA-CNPS, 84 p.
25. Li H-d, Yang C-r, Tian Z-y, Wu C-f, Qin W-q (2023) Cassiterite beneficiation in China: A mini-review. Journal of Central South University, 30(1): 1–19. https://doi.org/10.1007/s11771-023-5245-4
26. Li Q, Wang Y, Li Y, Li L, Tang M, Hu W, Chen L, Ai S (2022) Speciation of heavy metals in soils and their immobilization at micro-scale interfaces among diverse soil components. Science of the Total Environment, 825: 153862. https://doi.org/10.1016/j.scitotenv.2022.153862.
27. Li Z, Wang J, She Z, Gu J, Lu H, Wang S, He X, Yue Z (2024) Tailings particle size effects on pollution and ecological remediation: A case study of an iron tailings reservoir. Journal of Hazardous Materials, 476: 135024. https://doi.org/10.1016/j.jhazmat.2024.135024

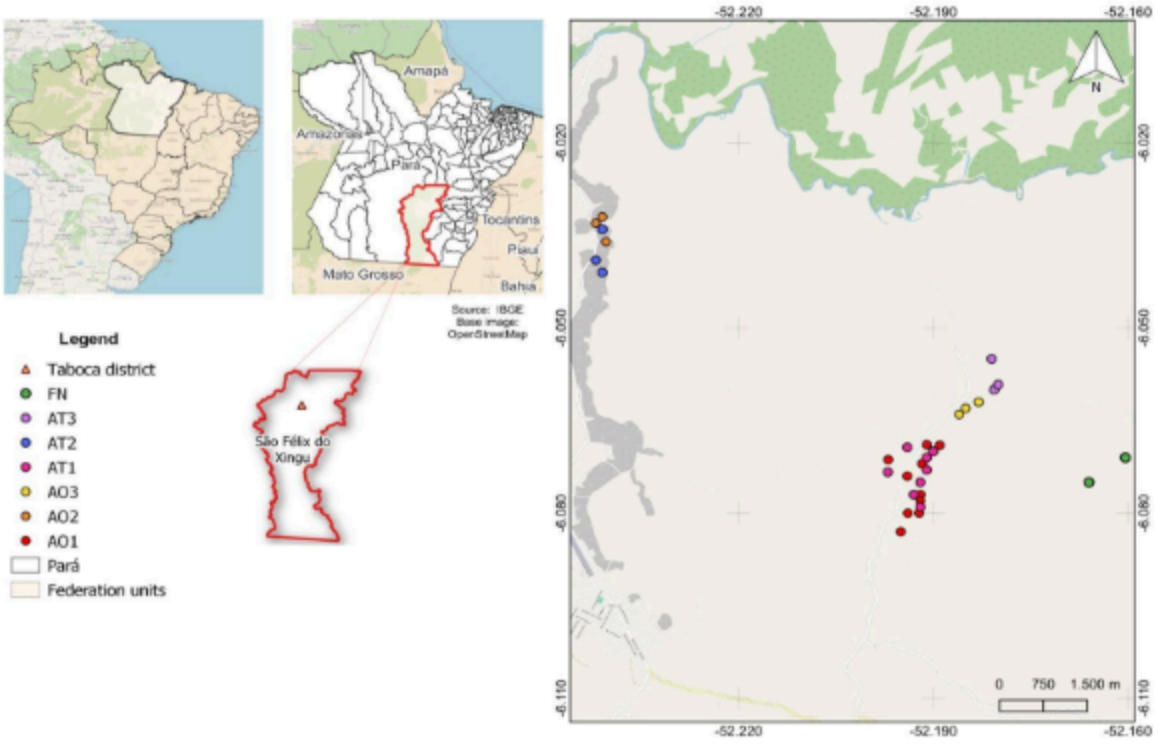
28. Lima AFL de, Campos MCC, Martins TS, Silva GA, Brito WBM, Santos LAC dos, Oliveira IA de, Cunha JM da (2022) Soil chemical attributes in areas under conversion from forest to pasture in southern Brazilian Amazon. Scientific Reports, 12(1): 22555. https://doi.org/10.1038/s41598-022-25406-9.
29. Mahecha-Pulido JD, Trujillo-González JM, Torres-Mora MA, García-Navarro FJ, Jiménez-Ballesta R (2025) Current status of acid soils under different landform types in an expanding equatorial agricultural region. Land, 14(5): 1073. https://doi.org/10.3390/land14051073
30. MapBiomas (2025) RAD2024: Relatório Anual do Desmatamento no Brasil 2024. São Paulo: MapBiomas, 209 p.
31. Martín D, Fernández-Caliani JC, Romero-Baena A, Delgado J, González I (2025) Geological constraints on the distribution of naturally occurring uranium and thorium in soils of southwestern Spain. Journal of Iberian Geology, 51: 445–461. https://doi.org/10.1007/s41513-025-00305-w
32. Melquiades FL, Bastos RO, Rampim L, Sandrino II, Rodriguez DG, Parreira PS (2024) Thorium and uranium rapid quantification in soil with portable X-ray fluorescence. Soil Science Society of America Journal, 88(2): 557–564. https://doi.org/10.1002/saj2.20639
33. Mitra A, Pandit SA, Azad S, Halliday AN (2025) Isotopic insights into redox processes driving uranium distribution in Eastern Karnataka groundwater. Environmental Science & Technology, 59(25): 12967–12977. https://doi.org/10.1021/acs.est.5c01913
34. Mogashane TM, Maree JP, Mokoena L, Tshilongo J (2025) Research activities on acid mine drainage treatment in South Africa (1998–2025): trends, challenges, bibliometric analysis and future directions. Water, 17(15): 2286. https://doi.org/10.3390/w17152286
35. Moia GCM, Matlaba VJ, Santos JF (2024) Evaluation of the impact of mining royalties on socio-environmental indicators in Parauapebas, Pará, the Eastern Amazon. The Extractive Industries and Society, 19: 101512. https://doi.org/10.1016/j.exis.2024.101512
36. Monicelli F, Cunha KPV, Araújo F, Becker V (2021) Phosphorus sorption potential of natural adsorbent materials from a Brazil semiarid region to control eutrophication. Acta Limnologica Brasiliensia, 33: e29. https://doi.org/10.1590/S2179-975X2621
37. Musiige D, Mundike J, Makondo C (2024) Evaluation of potentially toxic metals in tailings from Busia gold mine fields of eastern Uganda. Journal of Cleaner Production, 469: 143222. https://doi.org/10.1016/j.jclepro.2024.143222
38. Nahum ABR, Pereira WVS, Martins GC, Dias YN, Ribeiro PG, Salomão GN, Gastauer M, Caldeira CF, Fernandes AR, Souza ES de, Dall'Agnol R, Ramos SJ (2024) Properties and environmental quality of the overburden and tailings of manganese mining in the Eastern Amazon. Environmental Research, 262(2): 119965. https://doi.org/10.1016/j.envres.2024.119965
39. Nkinahamira F, Suanon F, Chi Q, Li Y, Feng M, Huang X, Yu CP, Sun Q (2019) Occurrence, geochemical fractionation, and environmental risk assessment of major and trace elements in sewage sludge. Journal of Environmental Management, 249: 109427. https://doi.org/10.1016/j.jenvman.2019.109427

40. Nwamba MN, Kelepile T, Ngatcha RB, Suh CE, Ilouga CDC, Shemang EM, Tantoh BS, Tata E, Agyingi CM (2023) Compositional provenance study of alluvial cassiterite at Bambol and Mayo Seni localities of the Mayo Darlé massif, northern Cameroon. Journal of Sedimentary Environments, 8(3): 311–338. https://doi.org/10.1007/s43217-023-00136-8
41. Otunola BO, Mhangara P (2024) Global advancements in the management and treatment of acid mine drainage. Applied Water Science, 14(9): 204. https://doi.org/10.1007/s13201-024-02259-3
42. Patel KS, Sharma SS, Maity JP, Martín-Ramos P, Fiket Ž, Bhattacharya P, Zhu Y (2023) Occurrence of uranium, thorium and rare earth elements in the environment: A review. Frontiers in Environmental Science, 10: 1058053. https://doi.org/10.3389/fenvs.2022.1058053
43. Pedrozo-Acuña A, Breña-Naranjo JA, Ramírez-Salinas N, Bustos-Montes JC, Soriano-Monzalvo JC, Zetina-Robleda EF, López-López MR (2025) Environmental impact of mining activities on water availability, quality and sediments in the Sonora River, Mexico. Water, Air, & Soil Pollution, 236(8): 524. https://doi.org/10.1007/s11270-025-08150-4
44. Pereira WVS, Ramos SJ, Melo LCA, Dias YN, Martins GC, Ferreira LCG, Fernandes AR (2023) Human and environmental exposure to rare earth elements in gold mining areas in the northeastern Amazon. Chemosphere, 340: 139824. https://doi.org/10.1016/j.chemosphere.2023.139824
45. Popoola OJ, Olubi OE, Adewalure OS, Raphael AE (2025) Elevated natural radionuclides in soils and stream sediments: pollution, spatial distribution, radiological hazards, and cancer risks in peri-urban Emure-Ekiti, southwest Nigeria. Discover Soil, 2(1): 70. https://doi.org/10.1007/s44378-025-00074-z
46. Porto JAM, Alves LJ, Medrado HHS, Rocha JS, Gois RGS, Nunes FC, Viana MM, et al. (2026) Determination of natural uranium and thorium levels in environmental matrices surrounding uranium mining sites via ICP-MS. Journal of Radioanalytical and Nuclear Chemistry, 335: 2533–2549. https://doi.org/10.1007/s10967-026-10785-4
47. Raso EF, Savaio SS, Mulima EP (2022) Impact of artisanal gold mining on agricultural soils: case of the district of Manica, Mozambique. Revista Verde de Agroecologia e Desenvolvimento Sustentável, 17(1): 44–50. https://doi.org/10.18378/rvads.v17i1.8486
48. Strawn DG (2021) Sorption mechanisms of chemicals in soils. Soil Systems, 5(1): 13. https://doi.org/10.3390/soilsystems5010013
49. Sutherland RA (2000) Bed sediment-associated trace metals in an urban stream, Oahu, Hawaii. Environmental Geology, 39: 611–627. https://doi.org/10.1007/s002540050473
50. Teixeira PC, Donagemma GK, Fontana A, Teixeira WG (2017) Manual de métodos de análise de solo. 3. ed. rev. e ampl. Brasília, DF: Embrapa, 574 p.
51. Veerasamy N, Murugan R, Kasar S, Inoue K, Kavasi N, Balakrishnan S, Arae H, Fukushi M, Sahoo SK (2021) Geochemical characterization of monazite sands based on rare earth elements, thorium and uranium from a natural high background radiation area in Tamil Nadu, India. Journal of Environmental Radioactivity, 232: 106565. https://doi.org/10.1016/j.jenvrad.2021.106565.
52. Vengosh A, Coyte RM, Podgorski J, Johnson TM (2022) A critical review on the occurrence and distribution of the uranium- and thorium-decay nuclides and their effect on the quality of

groundwater. Science of the Total Environment, 808: 151914. https://doi.org/10.1016/j.scitotenv.2021.151914.

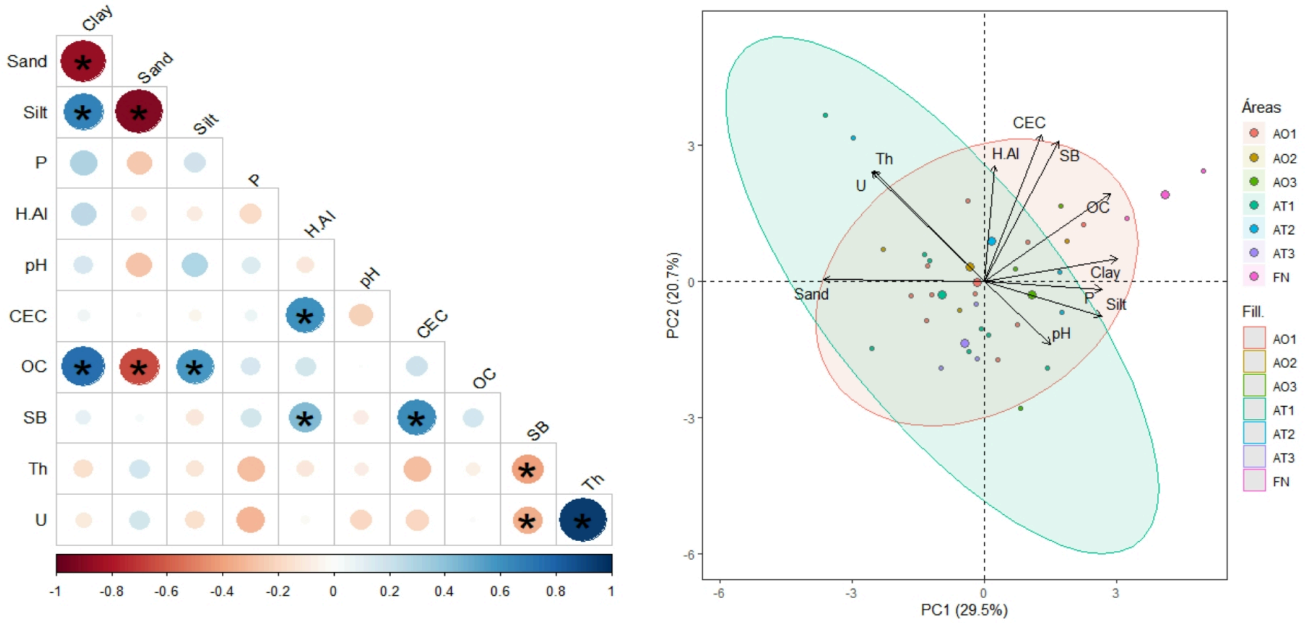
53. Wang B, Wang J, Pan Y, Xiao Y (2026) Research progress on rare earth extraction and recovery: A systematic review focusing on monazite concentrates decomposition technology from perspectives of environment and comprehensive recovery. Journal of Rare Earths. https://doi.org/10.1016/j.jre.2026.04.023.
54. Wang D, Hu L, Yang K, Huang S, Tian L (2024) Enhancement of U(VI) sorption in natural soils at prospective high-level radioactive waste geological disposal sites with $Fe(OH)_3$-humic acid composite colloids. Journal of Radioanalytical and Nuclear Chemistry, 333(3): 1203–1212. https://doi.org/10.1007/s10967-024-09369-x
55. Wang Z, Liu Z, Yu J, Wang Y, Zhou L (2021) Release behavior uranium and thorium in soil from a decommissioned uranium tailings in Jiangxi Province, China. Journal of Radioanalytical and Nuclear Chemistry, 330(3): 833–843. https://doi.org/10.1007/s10967-021-08030-1.
56. Wu D, Wang Y, Wang M, Wei C, Hu G, He X, Fu W (2021b) Basic characteristics of coal gangue in a small-scale mining site and risk assessment of radioactive elements for the surrounding soils. Minerals, 11(6): 647. https://doi.org/10.3390/min11060647
57. Wu W, Zhou J, Niu J, Lv H (2021a) Study on coupling between mineral resources exploitation and the mining ecological environment in Shanxi Province. Environment, Development and Sustainability, 23(9): 13261–13283. https://doi.org/10.1007/s10668-020-01209-8.
58. Xie T, Qian T, Lian B, Chen C, Liang P, Liu X, Zhu J (2024) Research on leaching behavior of uranium from a uranium tailing and its adsorption behavior in geotechnical media. Journal of Environmental Management, 353: 120207. https://doi.org/10.1016/j.jenvman.2024.120207
59. Xu Z, Yang J-L, Zhao Y, Hao R, Zhang G-L (2023) Soil acidification in a tailing area of ionic rare earth in Southeast China. Science of the Total Environment, 884: 163834. doi:10.1016/j.scitotenv.2023.163834.
60. Zhao P, Chen J, Liu T, Wang Q, Wu Z, Liang S (2023) Heavy metal pollution and risk assessment of tailings in one low-grade copper sulfide mine. Frontiers in Environmental Science, 11: 1132268. doi:10.3389/fenvs.2023.1132268.
61. Zhao T-Y, Li W-L, Kelebek S, Choi Y, Wu C-Q, Zhang W-J, Wang C-Y, Zhao Z-W, Sadri F (2025) A comprehensive review on rare earth elements: resources, technologies, applications, and prospects. Rare Metals, 44(10): 7011–7040. doi:10.1007/s12598-025-03459-9.

# Figures




## Figure 1

Artisanal monazite and cassiterite mining areas in the municipality of São Félix do Xingu




## Figure 2

Pearson correlation analysis (a) and principal component analysis (b) between sample properties and U and Th concentrations in the study areas

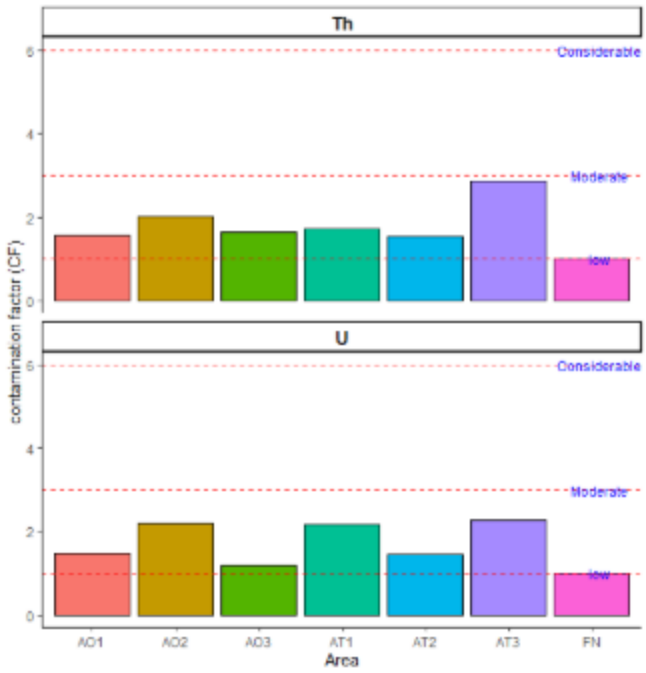



**Figure 3**

Contamination factor for U and Th in the study areas